Figure 6. (a) A comparison of the conformations of the monensin molecules as the free acid (light line) and the anhydrous sodium complex (this comparison was made by making a least-squares fit of the least flexible portion of the molecule [atoms C(4) to C(13) and O(4) to O-(6)]). (b) Differences in head-to-tail hydrogen bonding. (c) Differences in positions of oxygens of coordination.

changes in the O(1) to C(4) region internally compensate to leave the acid group little changed in relation to the reference fragment. The change in the C(13) to C(22) region on the other hand produces a concerted movement of oxygens O(8), O(9), and O(11) to bring them in position to coordinate incoming ions.

Complexation is almost certainly a process of sequential exchange of water of hydration for coordination to the oxygens of monensin. In the free acid the O(7) atom of the C ring is solvated, demonstrating it to be one of the most accessible of the coordinating oxygens. Complexation could easily be initiated by association of a metal ion with O(7). Two other oxygens, O(6) and

O(4), in the invariant position of the molecule, are positioned to displace additional water of hydration and induce a rearrangement in the hydrogen bonding, namely, the disruption of the hydrogen bond between O(6) and O(4) followed by the reversal of the donor–acceptor relationship in the O(4)–O(10) intramolecular hydrogen bond. This displacement of three solvent molecules by three coordinating oxygens requires no appreciable change in the conformation of monensin. In the transformation of the free acid to the complexed form, O(2) loses its acidic proton and accepts a hydrogen bond from O(10) while O(11) becomes a hydrogen bond donor to O(1). The disruption of the O(4)–O(6) hydrogen-bonding scheme appears to be the driving force for this rearrangement in head-to-tail hydrogen bonding. At the same time, small torsion angle changes permit O(8), O(9), and O(11) to move the 1–2 Å which is necessary to displace the remaining solvent from the metal ion and to complete the coordination.

The conformational change in the C ring and in the C(13)–O(7)–C(16)–C(17) torsion angle is the hinge upon which the molecular rearrangement turns. The flexibility of the C ring could be restricted by methyl substitution at C(14) or C(15). If the ability of monensin to complex metal ions is in part attributable to the flexibility of this ring, it may be possible to modify monensin's activity by such substitutions.

Supplementary Material Available: Tables of bond distances, bond angles, structure factors, atomic coordinates, and thermal parameters (38 pages). Ordering information is given on any current masthead page.

Imidazolate Complexes of Iron and Manganese Tetraphenylporphyrins

John T. Landrum,[1] K. Hatano,[2] W. Robert Scheidt,*[2] and Christopher A. Reed*[1]

Contribution from the Departments of Chemistry, University of Southern California, Los Angeles, California 90007, and University of Notre Dame, Notre Dame, Indiana 46556. Received February 6, 1980

Abstract: The possible importance of partially or completely deprotonated imidazole ligation in the hemoproteins has led us to investigate imidazolate, Im⁻, complexes of iron(II,III) and manganese(II,III) *meso*-tetraphenylporphyrin (TPP). Tetrabutylammonium imidazolate is a convenient reagent for the synthesis of isolable complexes. By steric and stoichiometric control the stereochemistry can be manipulated to give complexes with most possible coordination numbers and spin states. [Mn-(Im)₂(TPP)]⁻ is the first example of a low-spin Mn(III) porphyrin complex and demonstrates the greater ligand field strength of imidazolate over imidazole. The X-ray crystal structure of the polymer [Mn(Im)(TPP)]ₙ is reported. It shows layers of parallel chains with alternate layers having their quasi-linear chains approximately orthogonal to each other. There is a short–short/long–long alternation of Mn–N(Im) bond lengths (2.186 (5) and 2.280 (4) Å) interpreted as reflecting alternating predominantly low- and high-spin Mn(III) atoms along the polymeric chain. The average Mn–N(porph) bond distance is 2.019 (4) Å. Crystal data: $a = 20.073$ (3) Å, $b = 16.885$ (3) Å, $c = 22.590$ (5) Å, $\beta = 104.36$ (2)°, space group $C2/c$, $Z = 8$ (Mn(Im)(TPP) units).

Introduction

The ubiquity of "neutral" imidazole ligation to iron by histidine residues in the hemoproteins has led to speculation that partially or completely deprotonated imidazole ligation may also be im-

portant.[3-10] Imidazolate (Im⁻)[11] arises from complete deprotonation whereas hydrogen bonding of the N–H proton to bases

(3) Peisach, J. *Ann. N.Y. Acad. Sci.* **1975**, 244, 187–203.
(4) Chevion, M.; Salhany, J. M.; Peisach, J.; Castillo, C. L.; Blumberg, W. E. *Isr. J. Chem.* **1977**, 15, 311–317.
(5) Nappa, M.; Valentine, J. S.; Snyder, P. A. *J. Am. Chem. Soc.* **1977**, 99, 5799–5800.

(1) University of Southern California.
(2) University of Notre Dame.

6730 *J. Am. Chem. Soc., Vol. 102, No. 22, 1980*

Landrum et al.

(B) can in principle give rise to varying degrees of fractional deprotonation.

Fe	Fe	Fe
imidazole	H-bonded imidazole	imidazolate
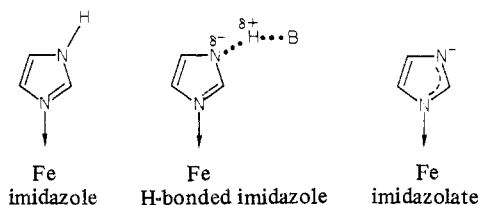
It may not be universally appreciated, but it is always the H-bonded imidazole structure which is observed in the hemoproteins whose structures have been published.[12] Thus, normally, histidyl imidazole ligands have developed more negative charge than a truly neutral imidazole. This has led us to conclude that "free" imidazole has a weaker field ligand than H-bonded imidazole and that this could serve as an explanation of the admixed-intermediate spin state of the cytochromes *c'*.[13] On the other hand, imidazolate is the extreme case of strong hydrogen bonding and imidazolate can be expected to be a stronger field ligand than neutral or H-bonded imidazole. This paper presents both structural and magnetic evidence that this is so. Other properties expected of mononuclear imidazolate porphyrin complexes (compared to imidazole complexes) are red-shifted Soret maxima,[6] shorter axial Fe–N bond distances, larger affinity constants especially to cationic metalloporphyrin centers,[14] and altered trans ligand-binding rates.[6,7] Further, the exo-bidentate ligand capacity of imidazolate to bridge two metal centers has led to speculation that it might mediate strong antiferromagnetic coupling between Cu(II) and Fe(III) at the heme a_3 site of cytochrome oxidase.[15] We do not, however, favor this role.[16]

To the best of our knowledge there are no reports of structurally characterized imidazolate complexes of metalloporphyrins and only one example of an isolated complex, [Fe(Im)(TPP)]$_m$,[17] other than those in our preliminary communication of this work.[18] In this paper we describe the synthetic methods developed to prepare convenient imidazolate reagents, show how coordination number, spin state, and stereochemistry can be manipulated in forming complexes with Fe(II), Fe(III), Mn(II), and Mn(III) porphyrins, give the full structural details for the polymer [Mn(Im)(TPP)]$_n$, and describe the magnetic, analytical, and spectroscopic data on these complexes.

(6) Mincey, T.; Traylor, T. G. *J. Am. Chem. Soc.* **1979**, *101*, 765–766.

(7) Swartz, J. C.; Stanford, M. A.; Moy, J. N.; Hoffman, B. M.; Valentine, J. S. *J. Am. Chem. Soc.* **1979**, *101*, 3396–3398.

(8) Brautigan, D. L.; Feinburg, B. A.; Hoffman, B. M.; Margoliash, E.; Peisach, J.; Blumberg, W. E. *J. Biol. Chem.* **1977**, *252*, 574–582.

(9) Valentine, J. S.; Sheridan, R. P.; Allen, L. C.; Kahn, P. *Proc. Natl. Acad. Sci. U.S.A.* **1979**, *76*, 1009–1013.

(10) Morrison, M.; Schonbaum, G. R. *Annu. Rev. Biochem.* **1976**, *45*, 861–888.

(11) Consistent abbreviation nomenclature which avoids confusion over the total charge on a species requires the use of Im⁻ when writing the free ligand but Im when writing a complex. For example: Im⁻ + FeCl(TPP) → Fe(Im)(TPP) + Cl⁻. Similarly, imidazole is written HIm which is consistent with the abbreviation of 1-MeIm for 1-methylimidazole. Other abbreviations used in this paper: TPP, dianion of tetraphenylporphyrin; 2-MeHIm, 2-methylimidazole; 2-MeIm⁻, 2-methylimidazolate anion; Bu₄N⁺, tetra-*n*-butylammonium cation; 4,5-DiPh-2-MeIm⁻, 4,5-diphenyl-2-methylimidazolate anion; THF = tetrahydrofuran.

(12) Salemme, F. R.; Freer, S. T.; Ng Huu Xuong; Alden, R. A.; Kraut, J. *J. Biol. Chem.* **1973**, *248*, 3910–3921.

(13) Reed, C. A.; Mashiko, T.; Bentley, S. P.; Kastner, M. E.; Scheidt, W. R.; Spartalian, K.; Lang, G. *J. Am. Chem. Soc.* **1979**, *101*, 2948–2958.

(14) (a) Walker, F. A.; Lo, M.-W.; Ree, M. T. *J. Am. Chem. Soc.* **1976**, *98*, 5552–5560. (b) Satterlee, J. D.; La Mar, G. N.; Frye, J. S. *Ibid.* **1976**, *98*, 7275–7282. (c) Balch, A. L.; Watkins, J. T.; Doonan, D. J. *Inorg. Chem.* **1979**, *18*, 1228–1231.

(15) Palmer, G.; Babcock, G. T.; Vickery, L. E. *Proc. Natl. Acad. Sci. U.S.A.* **1976**, *73*, 2206–2210.

(16) Reed, C. A.; Landrum, J. T. *FEBS Lett.* **1979**, *106*, 265–267.

(17) Cohen, I. A.; Ostfeld, D. *ACS Symp. Ser.* **1975**, *No. 5*, 221–233.

(18) Landrum, J. T.; Reed, C. A.; Hatano, K.; Scheidt, W. R. *J. Am. Chem. Soc.* **1978**, *100*, 3232–3234.

Experimental Section

Synthesis. All reactions were carried out in a Vacuum Atmospheres glovebox under He (H_2O, O_2 < 1 ppm). Solvents (AR grade) were dried and purified by distillation inside the glovebox from CaH_2 (heptane) or from purple sodium/benzophenone (THF, toluene, benzene). Ligands were AR grade and recrystallized from toluene before use. Room-temperature magnetic moments were measured on a Cahn 7600 Faraday system adapted for anaerobic work with an argon-flow glass-inlet tube and an internal polonium strip (Staticmaster, Nuclear Products Co.) to dispel static charge. Magnetic moments are corrected for diamagnetism by using Pascals' constants or experimentally measured diamagnetic susceptibilities using closely related diamagnetic models. Variable-temperature data were taken on a Faraday Balance at Bell Labs by courtesy of Frank DiSalvo. Spectra were recorded as follows: IR as KBr disks on a Perkin-Elmer 281, NMR on a Varian T60, and UV–VIS on a Beckman Acta MVI (tabulated in text). Fe(OClO₃)(TPP),[13] Fe(TPP),[19] Mn(TPP),[20] and MnCl(TPP)[21] were prepared by literature methods except that a new method for Fe(TPP) is reported.

Fe(TPP). FeCl(TPP) (1.0 g) and mercury-activated zinc pellets[20] were stirred in toluene (50 mL) until the visible spectrum indicated complete reduction (loss of λ_{max} = 511 nm). The solution was filtered through a medium or fine frit to remove the amalgum and ZnCl₂ byproduct, and the product was crystallized by the addition of heptane (0.9 g, 95%). The visible spectrum was identical with that of an authentic sample.[19]

Mn(OClO₃)(TPP)·2THF. MnCl(TPP) (265 mg) and AgClO₄ (74 mg) were warmed with stirring in tetrahydrofuran (15 mL) for 5 min. The solution was filtered through a fine frit, and green-black needles were deposited upon gradual addition of heptane (10 mL). Shock sensitivity of this perchlorate has not been observed, but caution is warranted when quantities larger than 50 mg are used. The yield of the 2THF solvate was 260 mg (90%): IR ν(ClO₄) 1120, 615 cm⁻¹; μ_{eff} = 5.1 μ_B (22 °C). Anal. Calcd for C₅₂H₄₄MnClO₆N₄: C, 68.57; H, 4.87; N, 6.15. Found: C, 68.98; H, 4.71; N, 6.11.

[Bu₄N][Im]. Imidazole (2 g) was dissolved in THF (200 mL), and NaH (0.7 g obtained from 1.28 g of heptane-washed 55% paraffin suspension) was slowly added. Once hydrogen evolution had ceased, the essentially quantitative yield of white precipitate of NaIm was filtered off and dried under vacuum. A typical product contained 0.3–0.5 equiv of occluded THF as measured by integration of the Im/THF proton ratio in the NMR spectrum in D₂O solution. This stoichiometry was taken into account when the weight of NaIm required was calculated in the following reaction. NaIm (1.55 g) and Bu₄NCl (5 g) in THF (150 mL) were stirred overnight. The white precipitate of NaCl was filtered off by using a medium frit, and heptane was added to the filtrate until cloudiness just persisted. The solvent was partially evaporated under vacuum, and the resulting cooling caused crystallization of the product. When a good yield was judged to have crystallized out, the off-white/colorless crystals of Bu₄NIm were filtered off and washed with heptane. NMR δ(D₂O): 0.93–1.81 (m, 28 H), 3.0 (m, 8 H), 6.95 (s, 2 H), 7.5 (s, 1 H). [Bu₄N][2-MeIm] was prepared in a similar manner. NMR δ(D₂O): 0.93–1.90 (m, 28 H), 2.3 (s, 3 H), 3.1 (m, 8 H), 6.9 (s, 2 H).

[Bu₄N][Fe^{III}(Im)₂(TPP)]. To Fe(OClO₃)(TPP)·0.5C₇H₈ (100 mg) in hot THF (20 mL) was added [Bu₄N][Im] (100 mg). After 2 min the solution was filtered to remove any solid impurities, and when the mixture stood, fine purple needles of product were deposited from the filtrate (90 mg, 70%). IR ν(C–H(Bu₄N)) 2950 (s), 2870 (m) cm⁻¹. Anal. Calcd for C₆₆H₇₀N₉Fe: C, 75.86; H, 6.76; N, 12.08. Found: C, 75.88; H, 6.70; N, 12.06. μ_{eff} = 2.5 μ_B (22 °C).

[Fe^{III}(Im)(TPP)·THF]$_n$. To a solution of Fe(OClO₃)(TPP)·0.5C₇H₈ (100 mg) in hot THF (30 mL) was added Bu₄NIm (38 mg). Rapid precipitation occurred, and the purple powder was filtered off and washed with THF (90 mg, 95%). Anal. Calcd for C₅₁H₃₉FeN₆O: C, 75.83; H, 4.87; N, 1.41. Found: C, 75.18; H, 4.36; N, 10.35. μ_{eff} = 2.5 μ_B (27 °C).

[Bu₄N][Mn^{III}(Im)₂(TPP)]. This was prepared in a manner identical with that of the Fe analogue above and isolated as fine dark green crystals. Anal. Calcd for C₆₆H₇₀N₉Mn: C, 75.78; H, 6.75; N, 12.04. Found: C, 76.09; H, 6.73; N, 12.06. μ_{eff} = 3.2 μ_B (25 °C).

[Mn^{III}(Im)(TPP)·THF]$_n$. This was prepared in a manner identical with that of the Fe analogue above and isolated as a black powder. Anal. Calcd for C₅₁H₃₉N₆OMn: C, 75.92; H, 4.87; N, 10.42. Found: C,

(19) Collman, J. P.; Hoard, J. L.; Kim, N.; Lang, G.; Reed, C. A. *J. Am. Chem. Soc.* **1975**, *97*, 2676–2681.

(20) Reed, C. A.; Kouba, J. K.; Grimes, C. J.; Cheung, S. K. *Inorg. Chem.* **1978**, *17*, 2666–2670.

(21) Adler, A. D.; Long, F. R.; Kampas, F.; Kim, J. *J. Inorg. Nucl. Chem.* **1970**, *32*, 2443–2445.

Table I. Summary of Crystal Data and Intensity Collection

formula	$C_{47}H_{31}N_6Mn$
fw, amu	734.745
a, Å	20.073 (3)
b, Å	16.885 (3)
c, Å	22.590 (5)
β, deg	104.36 (2)
V, Å^3	7417.4
Z	8
d, g/cm^3	1.316 (calcd)
	1.319 (obsd)
space group	$C2/c$
cryst dimens	0.50 × 0.55 × 0.40 mm
temp, °C	20 ± 1
radiatn	graphite-monochromated Mo Kα
	($\bar{\lambda}$ = 0.710 73 Å)
μ, mm^{-1}	0.384
scan type	θ–2θ
scan range	0.7° below Kα_1
	to 0.7° above Kα_2
scan rates	2–12°/min
2θ limits	3.5–54.9
bkgd counts	extreme of scans for $^1/_2$
	time of scan
p	0.04
unique data with $F_o > 3\sigma(F_o)$	4320

75.60; H, 4.86; N, 9.93. NMR integration solvate analysis from trifluoroacetic acid decomposition: calcd for THF, 8.9; found, 9.8. Single crystals of nonsolvated [Mn(Im)(TPP)]$_n$ were prepared as follows. "Mn(TPP)(OH)" was prepared by the reaction of H$_2$TPP with Mn(O-Ac)$_2$ in DMF, precipitation with NaOH/H$_2$O, and recrystallization (twice) from CH$_3$OH/H$_2$O.[21] A solution of CH$_3$OH/NaOCH$_3$ (20 mL) (prepared by adding sodium (~100 mg) to CH$_3$OH (50 mL)), CH$_3$OH (10 mL), and a saturated solution of "Mn(TPP)(OH)" (10 mL) containing imidazole (10 mg) was carefully layered and allowed to stand for several days. The resulting crystals were washed with water and air-dried. Anal. Calcd for C$_{47}$H$_{31}$N$_6$Mn: C, 76.83; H, 4.25; N, 11.44. Found: C, 76.53; H, 4.20; N, 11.33.

[Bu$_4$N][Mn^{II}(Im)(TPP)]·THF. To a purple-green solution of Mn(T-PP)·2C$_7$H$_8$ (200 mg) in hot THF (25 mL) was added Bu$_4$NIm (43 mg). The resulting bright green solution was filtered through a medium frit, and upon cooling of the solution and gradual addition of heptane large, purple crystals were deposited (170 mg, 75%). IR ν(C–H(Bu$_4$N)) 2950 (s), 2870 (m) cm^{-1}. Anal. Calcd for C$_{67}$H$_{75}$N$_7$OMn: C, 76.66; H, 7.20; N, 9.34. Found: C, 76.16; H, 6.79; N, 9.77. μ_{eff} = 6.4 μ_B (25 °C).

[Bu$_4$N]Fe^{II}(2-MeIm)(TPP)]. To a hot solution of Fe(TPP) (200 mg) in toluene (50 mL) was added [Bu$_4$N][2-MeIm] (43 mg). As soon as the reactant was dissolved, the hot solution was quickly filtered and the product crystallized by addition of heptane. IR ν(C–H(Bu$_4$N)) 2950 (s), 2870 (m) cm^{-1}. μ_{eff} = 5.0 μ_B. Anal. Calcd for C$_{64}$H$_{69}$N$_7$Fe: C, 77.42; H, 6.96; N, 9.87. Found: C, 76.62; H, 6.90; N, 9.42.

Fe^{III}(4,5-DiPh-2-MeIm)(TPP). To a solution of Fe(OClO$_3$)(TPP)·0.5C$_7$H$_8$ (400 mg) in toluene (40 mL) was added sodium 4,5-diphenyl-2-methylimidazolate (125 mg, prepared in a manner identical with that of NaIm described above). The solution was stirred for 5 min and then filtered through a medium frit. Heptane was added to the filtrate to induce crystallization. The purple crystalline product was filtered off and washed with toluene (150 mg, 30%). IR showed absence of perchlorate and μ-oxo dimer products which contaminate the product if the solvents are not scrupulously dry. Anal. Calcd for C$_{60}$H$_{41}$N$_6$Fe: C, 79.8; H, 4.54; N, 9.3. Found: C, 79.62; H, 4.9; N, 8.83. μ_{eff} = 6.2 μ_B (25 °C).

X-ray Structure Determination. Preliminary examination of a single crystal of [Mn(Im)(TPP)]$_n$ by precession photography with Cu Kα radiation demonstrated a C-centered monoclinic unit cell with eight C$_{47}$-H$_{31}$N$_6$Mn units. The systematic absences are consistent with Cc or $C2/c$ as the possible space groups. Precise lattice constants were obtained from the setting angles of 60 reflections, collected at ±2θ, and led to the cell constants reported in Table I.

Intensity data were measured on a Syntex P1̄ diffractometer; a summary of the intensity collection values is given in Table I. Four standard reflections were measured every 50 reflections during data collection to monitor the long-term stability; no significant deviations were observed. Intensity data were reduced and standard deviations calculated as described previously.[22] A total of 4320 reflections had $F_o > 3\sigma(F_o)$ and were used in all subsequent calculations.

The structure was solved by the heavy-atom method[23] and refined by block-diagonal and full-matrix least-squares techniques.[24] A Patterson calculation did not reveal Mn–Mn vectors in the expected general positions in the space group $C2/c$. Rather the Patterson map was consistent only with Mn atom positions of $^1/_4,^1/_4,^1/_2$ and $^1/_2,^1/_2,^1/_2$ in space group $C2/c$. In space group Cc, the Mn atoms must be separated by the rather special condition of $^1/_4,^1/_4,0$. Note that for *either* choice of space group, there are two crystallographically distinct Mn atoms. Initial structure solution was commenced by assuming the correct space group was $C2/c$ with the two independent Mn atoms located on inversion centers. Thus, the crystallographically unique atoms are two half [Mn(TPP)]$^+$ ions and an imidazole (C$_3$H$_3$N$_2^-$) ion. A series of difference Fourier calculations served to provide initial coordinates of all atoms. Least-square refinement was then commenced. An isotropic refinement converged at relatively high values of the discrepancy indices. A difference Fourier showed electron density maxima appropriately located for many hydrogen atoms of the two porphinato ligands and also a large number of peaks associated with the two independent phenyl rings of the porphinato ligand coordinated to Mn$_2$. When anisotropic refinement of these two phenyl rings was attempted, the thermal parameters were quite anisotropic and physically unrealistic. An examination of a difference Fourier synthesis, from which the two phenyl rings were omitted, suggested that each phenyl ring had two different orientations. Relative peak heights were consistent with occupancies of ~2.5:1 for each pair of disordered phenyl groups. There was no evidence for this type of disorder associated with the phenyl rings of the other independent porphinato ligand. These disorder problems might suggest an incorrect choice of space group, but attempted refinement in Cc was unsuccessful. It should be noted that the orientations of the disordered phenyl rings must be correlated over the symmetry positions within any given unit cell in order to avoid unrealistically close nonbonded contacts. The phenyl groups were refined as rigid groups. The geometry observed for the phenyl groups of the low-temperature Mn(TPP) structure[25] was employed for the rigid-group description. The occupancy factors for each pair of disordered phenyl rings were refined subject to the constraint that the sum equals 1.0; the final occupancy factors were 0.75 and 0.25 and 0.69 and 0.31. The presence of the disordered phenyl rings is possibly related to structural changes from the spin equilibrium of the predominantly low-spin manganese atom, Mn$_1$ (vide infra). The atoms of the disordered phenyl groups were assigned individual isotropic temperature factors. An ORTEP plot of the disorder model employed is given in the supplementary material (Figure 5). The remaining atoms were allowed anisotropic temperature factors; hydrogen atoms of the two porphinato ligands and the imidazolate ligand were assigned to their theoretically calculated positions (C–H = 0.95 Å) with isotropic temperature factors fixed one unit higher than those of the associated carbon atom. Hydrogen atom contributions were then included as fixed contributors to the remaining cycles of least-squares refinement.

Final least-squares refinement led to final residuals of $R_1 = \sum (|F_o| - |F_c|)/\sum|F_o|$ of 0.090 and $R_2 = [\sum w(|F_o| - |F_c|)^2/\sum w(F_o)^2]^{1/2}$ of 0.089, an error of fit of 2.08 and a final data/parameter ratio of 10.6. A final difference Fourier was essentially featureless with a peak of 0.65 e/Å^3 near Mn$_2$ and smaller peaks (<~0.35 e/Å^3) elsewhere in the map. A final listing of the observed and calculated structure factor amplitudes is available as supplementary material.

The final atomic coordinates and associated anisotropic thermal parameters for the nongroup atoms are given in Tables II and III, respectively. The derived atomic coordinates of the phenyl rings and their associated thermal parameters are given in Table IV (supplementary material).

Description of the [Mn(Im)(TPP)]$_n$ Structure. A perspective view of three units of the [Mn(Im)(TPP)]$_n$ polymeric chain is shown in Figure 1. The lower two centrosymmetric [Mn(TPP)]$^+$ units and one bridging imidazolate ion are the crystallographically unique portion of the polymer. Also displayed in Figure 1 are the bond distances of the coordinated atoms to the two Mn(III) atoms and the bond distances and angles of the imidazolate anion. A particularly curious feature of the structure is

(22) Scheidt, W. R. *J. Am. Chem. Soc.* **1974,** *96,* 84–90.

(23) A locally modified version of the Fourier program ALFF was used: Hubbard, C. R.; Quicksall, C. O.; Jacobson, R. A. Report 15-2625; Ames Laboratory: Iowa State University, Ames, IA, 1971.

(24) Locally modified versions of REFINE by J. J. Park and ORFLS by Busing, Levy, and Martin were used. Atomic form factors were from: Cromer, D. T.; Mann, J. B. *Acta Crystallogr., Sect. A* **1968,** *24A,* 321–324, with real and imaginary corrections for anomalous scattering in the form factor of the manganese atom from: Cromer, D. T.; Liberman, D. *J. Chem. Phys.* **1970,** *53,* 1891–1898. Scattering factors for hydrogen were from: Stewart, R. F.; Davidson, E. R.; Simpson, W. T. *J. Chem. Phys.* **1965,** *42,* 3175–3187.

(25) Kirner, J. F.; Reed, C. A.; Scheidt, W. R. *J. Am. Chem. Soc.* **1977,** *99,* 1093–1101.

Table II. Atomic Coordinates in the Unit Cell[a]

atom type	$10^4 x$	$10^4 y$	$10^4 z$
Mn_1	1/4	1/4	1/2
Mn_2	1/2	1/2	1/2
NI_1	3125 (2)	3558 (3)	4993 (2)
NI_2	3974 (2)	4423 (3)	5002 (2)
CI_1	3791 (3)	3690 (3)	5063 (3)
CI_2	3378 (4)	4796 (4)	4865 (5)
CI_3	2864 (3)	4274 (4)	4847 (5)
N_1	2071 (2)	2650 (3)	4096 (2)
N_2	1741 (2)	3152 (2)	5195 (2)
N_3	5539 (2)	4209 (3)	5603 (2)
N_4	5049 (2)	4275 (3)	4302 (2)
C_{a1}	2327 (3)	2371 (3)	3619 (3)
C_{b1}	1886 (4)	2642 (4)	3055 (3)
C_{b2}	1365 (3)	3041 (4)	3183 (3)
C_{a2}	1487 (3)	3061 (4)	3837 (3)
C_{a3}	1207 (3)	3502 (3)	4786 (3)
C_{b3}	793 (3)	3935 (4)	5109 (3)
C_{b4}	1070 (3)	3823 (4)	5705 (3)
C_{a4}	1663 (3)	3331 (3)	5773 (3)
C_{m1}	1074 (3)	3454 (3)	4153 (3)
C_{m2}	2920 (3)	1924 (3)	3676 (3)
C_{a5}	5791 (3)	4313 (4)	6218 (3)
C_{b5}	6228 (3)	3672 (4)	6474 (3)
C_{b6}	6246 (3)	3186 (4)	6012 (3)
C_{a6}	5821 (3)	3508 (3)	5460 (3)
C_{a7}	5392 (3)	3570 (4)	4343 (3)
C_{b7}	5288 (4)	3235 (5)	3740 (3)
C_{b8}	4885 (4)	3733 (5)	3345 (3)
C_{a8}	4736 (3)	4388 (4)	3692 (3)
C_{m3}	5751 (3)	3204 (3)	4879 (3)
C_{m4}	4325 (3)	5033 (4)	3442 (3)

[a] The numbers in parentheses are the estimated standard deviation in the last significant figure.
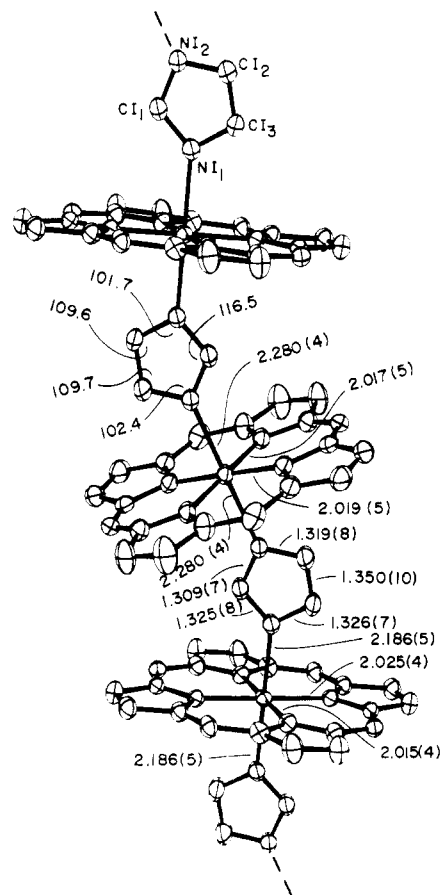

Figure 1. A ORTEP plot of three units of the $[Mn(Im)(TPP)]_n$ polymer. Each Mn(III) atom is located at an inversion center; the lowest two units (with required C_i-$\bar{1}$ symmetry) are the crystallographically unique portion of the polymer. For clarity, the peripheral phenyl groups are omitted. Bond distances in the coordination group and bond distances and angles for the imidazolate ligand are entered on the diagram.

the short–short/long–long alternation of Mn–N(Im) bond distances (to Mn_1 and Mn_2, respectively) in the chain, a point for subsequent discussion.

Figure 1 clearly displays the zigzag nature of the chain; with the required C_i-$\bar{1}$ site symmetry for each Mn(III) atom, the two axial N-

Table III. Thermal Parameters[a]

atom type	B_{11}	B_{22}	B_{33}	B_{12}	B_{13}	B_{23}
Mn_1	3.37 (5)	2.71 (5)	4.04 (6)	−0.13 (5)	1.69 (5)	0.01 (5)
Mn_2	3.27 (5)	3.48 (6)	5.13 (7)	0.54 (5)	1.72 (5)	0.56 (5)
NI_1	4.1 (2)	3.5 (2)	5.4 (3)	0.6 (2)	1.7 (2)	0.2 (2)
NI_2	3.8 (2)	3.5 (2)	6.4 (3)	0.6 (2)	1.9 (2)	0.4 (2)
CI_1	4.2 (3)	3.5 (3)	7.1 (4)	1.0 (2)	2.1 (3)	0.8 (3)
CI_2	4.5 (4)	3.7 (4)	21.0 (10)	0.9 (3)	3.9 (5)	2.5 (5)
CI_3	3.4 (3)	4.0 (4)	22.9 (10)	0.9 (3)	3.8 (5)	2.1 (5)
N_1	3.6 (2)	3.8 (2)	4.0 (2)	0.0 (2)	1.7 (2)	0.0 (2)
N_2	3.1 (2)	3.2 (2)	4.0 (2)	0.0 (2)	1.5 (2)	−0.2 (2)
N_3	3.2 (2)	4.1 (2)	5.5 (3)	0.3 (2)	1.4 (2)	0.5 (2)
N_4	3.7 (2)	4.0 (2)	5.2 (3)	0.8 (2)	1.8 (2)	0.4 (2)
C_{a1}	4.9 (3)	4.0 (3)	3.6 (3)	0.3 (2)	1.5 (2)	0.2 (2)
C_{b1}	7.1 (4)	6.8 (4)	4.6 (4)	2.3 (3)	2.4 (3)	0.1 (3)
C_{b2}	5.9 (4)	6.5 (4)	4.6 (4)	2.2 (3)	1.5 (3)	0.3 (3)
C_{a2}	4.5 (3)	3.9 (3)	4.0 (3)	0.3 (2)	1.6 (2)	0.1 (2)
C_{a3}	3.1 (2)	3.0 (2)	4.5 (3)	−0.1 (2)	1.5 (2)	−0.2 (2)
C_{b3}	3.9 (3)	5.1 (3)	4.7 (3)	1.2 (3)	1.2 (3)	0.3 (3)
C_{b4}	4.5 (3)	4.7 (3)	5.6 (4)	0.6 (3)	2.6 (3)	−0.2 (3)
C_{a4}	3.8 (3)	3.6 (3)	4.8 (3)	0.3 (2)	2.0 (2)	0.2 (2)
C_{m1}	3.6 (3)	3.4 (3)	4.8 (3)	0.1 (2)	1.4 (2)	0.3 (2)
C_{m2}	4.4 (3)	3.7 (3)	4.4 (3)	0.7 (2)	2.3 (2)	0.1 (2)
C_{a5}	4.1 (3)	4.8 (3)	6.0 (4)	0.3 (3)	1.4 (3)	0.8 (3)
C_{b5}	4.9 (3)	5.9 (4)	5.7 (4)	0.5 (3)	0.3 (3)	1.1 (3)
C_{b6}	4.7 (3)	3.9 (3)	8.3 (5)	0.4 (3)	−0.3 (3)	1.5 (3)
C_{a6}	3.0 (3)	3.7 (3)	6.3 (4)	−0.4 (2)	1.0 (3)	0.7 (3)
C_{a7}	4.2 (3)	4.4 (3)	6.3 (4)	0.3 (3)	2.3 (3)	0.0 (3)
C_{b7}	8.3 (5)	7.9 (5)	6.7 (5)	3.5 (4)	3.4 (4)	−1.0 (4)
C_{b8}	10.2 (6)	9.5 (5)	5.1 (4)	3.9 (5)	2.9 (4)	0.0 (4)
C_{a8}	5.9 (4)	6.1 (4)	5.6 (4)	1.6 (3)	2.2 (3)	0.1 (3)
C_{m3}	3.6 (3)	3.1 (3)	7.3 (4)	−0.2 (2)	1.5 (3)	−0.4 (3)
C_{m4}	5.4 (3)	7.6 (4)	4.5 (3)	1.0 (3)	1.1 (3)	1.0 (3)

[a] B_{ij} is related to the dimensionless β_{ij} employed during refinement as $B_{ij} = 4\beta_{ij}/a_i^* a_j^*$.
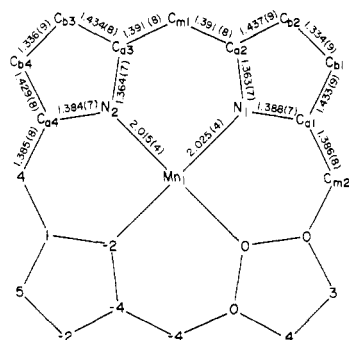
Figure 2. A formal diagram of the porphinato core of one [Mn(TPP)]$^+$ unit of [Mn(Im)(TPP)]$_n$, displaying, on the upper half, the structurally independent bond lengths and the numbering scheme employed for the atoms. On the lower half of the centrosymmetric diagram, the numbered symbol for each atom is replaced by its perpendicular displacement, in units of 0.01 Å, from the mean plane of the porphinato core.
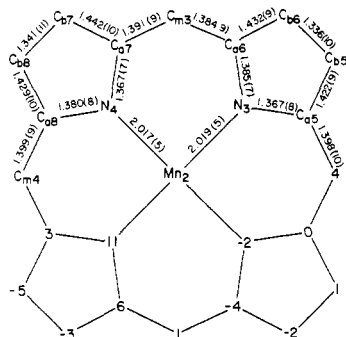
Figure 3. A formal diagram of the porphinato core of the other [Mn(TPP)]$^+$ unit of the [Mn(Im)(TPP)]$_n$ polymer displaying the same information as in Figure 2.

(Im)–Mn–N(Im) bond angles are 180.0°. The intrachain Mn–Mn separations are 6.56 Å; the interchain Mn–Mn separations are greater than 11 Å. The zigzag character of the chain results from the bonding requirements of the imidazolate ligand; however, the geometry deviates significantly from ideality. The dihedral angle between the mean planes of adjacent porphinato cores is 28.5°, to be compared to an expected value of ~38.5° if the Mn–N(Im) bond vectors bisected the respective C–N–C angles of imidazolate and were perpendicular to their respective porphinato plane. The decrease in the dihedral angle is accomplished by tipping the Mn–N(Im) vectors from the normal to the porphinato planes (Mn–N$_1$ is tipped 1.6° and Mn$_2$–N$_2$ by 6.5°) and unequal Mn–N–C(Im) angles. Presumably, the decrease in the porphinato plane dihedral angle is required to minimize nonbonded contacts between the porphinato ligands. The dihedral angle between the imidazolate plane and the porphinato plane 1 (Mn$_1$) is 86.3° and the porphinato plane 2 (Mn$_2$) is 80.3°. While the imidazolate ring is planar to within 0.015 Å, Mn$_1$ and Mn$_2$ are 0.07 and 0.17 Å, respectively, out of the imidazolate plane. The imidazolate plane forms angles of 26 and 28° with coordinate planes of the two porphinato cores.

Figures 2 and 3 present the values for the individual bond distances in the porphinato cores as well as displaying the numbering scheme employed for the angles tabulated in Table V. Averaged values for the chemically equivalent bond distances and angles are presented in Table VI. The average Mn–N(porph) bond distance of 2.019 (4) Å compares well with those observed in other six-coordinate (porphinato)manganese(III) derivatives: 2.015 (4) Å in [Mn(1-MeIm)$_2$(TPP)]ClO$_4$,[26] 2.009 (9) Å in Mn(Cl)(py)(TPP),[27] and 2.031 (12) Å in Mn(N$_3$)(CH$_3$OH)-(TPP).[28] The geometry for the bridging imidazolate in [Mn(Im)(TPP)]$_n$ is in general agreement with those observed previously.[29] A general

(26) Steffen, W. L.; Chun, H. K.; Hoard, J. L.; Reed, C. A. "Abstracts of Papers", 175th National Meeting of the American Chemical Society, Anaheim, CA, March, 1978; American Chemical Society: Washington, D.C., 1978; INOR 15.

(27) Kirner, J. F.; Scheidt, W. R. *Inorg. Chem.* **1975**, *14*, 2081–2086.

(28) Day, V. W.; Stults, B. R.; Tasset, E. L.; Day, R. O.; Marianelli, R. S. *J. Am. Chem. Soc.* **1974**, *96*, 2650–2652.

(29) O'Young, C.-L.; Dewan, J. C.; Lilienthal, H. R.; Lippard, S. J. *J. Am. Chem. Soc.* **1978**, *100*, 7291–7300. Lundberg, B. K. S. *Acta Chem. Scand.* **1972**, *26*, 3902–3911 and references therein.

Table V. Bond Angles in the Coordination Group, Porphinato Skeleton, and Imidazolate Ligand

angle[a]	value, deg	angle[a]	value, deg
$N_1Mn_1N_2$	89.8 (2)	$C_{a5}C_{b5}C_{b6}$	106.4 (6)
$N_3Mn_2N_4$	90.2 (2)	$C_{a6}C_{b6}C_{b5}$	108.8 (6)
$N_1Mn_1NI_1$	89.5 (2)	$C_{a7}C_{b7}C_{b8}$	107.7 (6)
$N_2Mn_1NI_1$	88.8 (2)	$C_{a8}C_{b8}C_{b7}$	107.1 (6)
$N_3Mn_2NI_2$	87.2 (2)	$C_{a2}C_{m1}C_{a3}$	124.7 (5)
$N_4Mn_2NI_2$	87.8 (2)	$C_{a4}''C_{m2}C_{a1}$	124.5 (5)
$C_{a1}N_1C_{a2}$	106.4 (4)	$C_{a6}C_{m3}C_{a7}$	124.8 (5)
$C_{a3}N_2C_{a4}$	106.9 (4)	$C_{a8}C_{m4}C_{a5}''$	123.8 (6)
$C_{a5}N_3C_{a6}$	106.0 (5)	$C_{a2}C_{m1}C_1$	117.4 (5)
$C_{a7}N_4C_{a8}$	106.5 (5)	$C_{a3}C_{m1}C_1$	117.9 (4)
$N_1C_{a1}C_{b1}$	108.4 (5)	$C_{a4}''C_{m2}C_7$	117.0 (4)
$N_1C_{a2}C_{b2}$	109.9 (5)	$C_{a1}C_{m2}C_7$	118.4 (5)
$N_2C_{a3}C_{b3}$	109.5 (5)	$C_{a6}C_{m3}C_{13}$	119.7 (5)
$N_2C_{a4}C_{b4}$	108.2 (5)	$C_{a7}C_{m3}C_{13}$	115.5 (5)
$N_3C_{a5}C_{b5}$	110.7 (5)	$C_{a6}C_{m3}C_{13}'$	102.5 (5)
$N_3C_{a6}C_{b6}$	108.1 (5)	$C_{a7}C_{m3}C_{13}'$	132.8 (5)
$N_4C_{a7}C_{b7}$	109.0 (6)	$C_{a8}C_{m4}C_{19}$	113.6 (5)
$N_4C_{a8}C_{b8}$	109.7 (6)	$C_{a5}''C_{m4}C_{19}$	121.6 (5)
$N_1C_{a1}C_{m2}$	125.8 (5)	$C_{a8}C_{m4}C_{19}'$	121.6 (5)
$N_1C_{a2}C_{m1}$	125.5 (5)	$C_{a5}''C_{m4}C_{19}'$	113.2 (5)
$N_2C_{a3}C_{m1}$	126.2 (5)	$CI_1NI_1CI_3$	101.7 (5)
$N_2C_{a4}C_{m2}''$	126.5 (5)	$CI_1NI_2CI_2$	102.4 (5)
$N_3C_{a5}C_{m4}''$	126.1 (5)	$NI_1CI_2NI_2$	116.5 (5)
$N_3C_{a6}C_{m3}$	125.9 (5)	$NI_2CI_2CI_3$	109.7 (6)
$N_4C_{a7}C_{m3}$	126.1 (6)	$NI_1CI_3CI_2$	109.6 (6)
$N_4C_{a8}C_{m4}$	126.0 (6)	$Mn_1NI_1CI_1$	134.4 (4)
$C_{m2}C_{a1}C_{b1}$	125.8 (5)	$Mn_1NI_1CI_3$	123.6 (4)
$C_{m1}C_{a2}C_{b2}$	124.6 (5)	$Mn_2NI_2CI_1$	133.0 (4)
$C_{m1}C_{a3}C_{b3}$	124.4 (5)	$Mn_2NI_2CI_2$	124.3 (4)
$C_{m2}''C_{a4}C_{b4}$	125.4 (5)	$Mn_1N_1C_{a1}$	126.5 (4)
$C_{m4}''C_{a5}C_{b5}$	123.1 (6)	$Mn_1N_1C_{a2}$	127.1 (3)
$C_{m3}C_{a6}C_{b6}$	125.8 (6)	$Mn_1N_2C_{a3}$	126.7 (3)
$C_{m3}C_{a7}C_{b7}$	124.8 (6)	$Mn_1N_2C_{a4}$	126.4 (4)
$C_{m4}C_{a8}C_{b8}$	124.3 (6)	$Mn_2N_3C_{a5}$	127.0 (4)
$C_{a1}C_{b1}C_{b2}$	108.4 (5)	$Mn_2N_3C_{a6}$	126.2 (4)
$C_{a2}C_{b2}C_{b1}$	106.9 (6)	$Mn_2N_4C_{a7}$	126.7 (4)
$C_{a3}C_{b3}C_{b4}$	106.9 (5)	$Mn_2N_4C_{a8}$	126.8 (4)
$C_{a4}C_{b4}C_{b3}$	108.5 (5)		

[a] C_i and C_i' represent the atom pairs in the two disordered phenyl groups. C_i and C_i'' denote atoms related by the inversion centers at Mn_1 and Mn_2.

Table VI. Average Bond Distances and Angles in the Porphinato Cores[a]

	A. Bond Distances, Å		
C_a–N	1.375 (10)	C_a–C_m	1.391 (6)
C_a–C_b	1.432 (6)	C_b–C_b	1.337 (3)
Mn–N	2.019 (4)		

	B. Bond Angles, Deg		
C_aNC_a	106.4 (4)	NC_aC_b	126.7 (3)
$C_aC_bC_b$	107.6 (9)	NC_aC_m	126.0 (3)
$MnNC_a$	126.7 (3)		

[a] The estimated standard deviation is calculated on the assumption that all averaged values are drawn from the same population.

feature of ligated imidazolate relative to ligated imidazole is an increase in the internal angles at carbon and a decrease in the internal angles at nitrogen; these features appear a bit more pronounced in the present case.

The relative arrangement of the chains can be described as layers of quasi-parallel chains with alternate layers having the chains approximately orthogonal to each other. This can be readily visualized by specifying the coordinates of the Mn(III) atoms in one chain ($z = \frac{1}{2}$ layer) $0,0,\frac{1}{2}$, $\frac{1}{4},\frac{1}{4},\frac{1}{2}$, $\frac{1}{2},\frac{1}{2},\frac{1}{2}$, etc. and $\frac{3}{4},\frac{1}{4},0,\frac{1}{2},\frac{1}{2},0,\frac{1}{4},\frac{3}{4},0$, etc. in the chain of the parallel ($z = 0$) layer.

Discussion

The general synthetic strategy with the imidazolate ion derivatives reported herein was to choose salt solubilities which made product isolation clean and straightforward. The tetra-*n*-butylammonium imidazolates were not only useful in this regard but also, the greatly increased effective molecular weight of the imidazolate facilitated weighing exact stoichiometries.

Table VII. Comparison of visible spectral Maxima for Various Imidazolate and Imidazole Complexes

complex[b]		solvent	principal Soret max, nm ($10^{-4}\epsilon$, L mol^{-1} cm^{-1})	other maxima, nm ($10^{-4}\epsilon$, L mol^{-1} cm^{-1})
Bu$_4$N	[Fe^{III}(Im)$_2$(TPP)]	THF	424 (9.2)	442 sh (0.84), 555 (0.11), 602 (0.01)
	[Fe^{III}(ImH)$_2$(TPP)][ClO$_4$][a]	THF	415 (16.5)	457 sh (1.7), 547 (1.2), 580 (0.7)
	[Fe^{III}(2-Me-4,5-Ph$_2$Im)(TPP)][c]	TOL	413 (9.5)	373 sh, 570 (0.72), 608 (0.35)
[Bu$_4$N]$_2$	[Fe^{II}(Im)$_2$(TPP)]	THF	445 (6.3)	365 sh, 504 sh, 547 (1.6), 580 sh, 614 (0.23)
	[Fe^{II}(ImH)$_2$(TPP)][a]	THF	425 (30.0)	404 sh, 532 (2.4), 563 (0.6)
Bu$_4$N	[Fe^{II}(2-MeIm)(TPP)]	THF	446 (11.0)	400 sh, 530 (0.7), 573 (1.7), 614 (1.5)
	[Fe^{II}(2-MeImH)(TPP)][a]	THF	434 (17.5)	367 (1.9), 530 (1.0), 561 (1.0), 609 (0.6)
Bu$_4$N	[Mn^{III}(Im)$_2$(TPP)]	THF	450 (2.9)	390 sh, 410 (2.0), 425 sh, 460 sh, 498 (0.68), 540 (0.18), 588 (0.30), 628 (0.47)
	[Mn^{III}(ImH)$_2$(TPP)]ClO$_4$[a]	THF	473 (5.6)	376 (2.7), 400 (2.7), 424 (1.8), 525 (0.63), 571 (1.1), 608 (1.0)
	[Mn^{III}(2-Me-4,5-Ph$_2$Im)(TPP)]	TOL	412 (1.1)	380 sh, 472 (0.83), 530 (2.20), 579 (0.15), 618 (0.13)
Bu$_4$N	[Mn^{II}(Im)(TPP)]	THF	448 (11.5)	408 (10), 540 (0.4), 580 (1.2), 625 (1.9)
	[Mn^{II}(ImH)(TPP)]	THF	439 (42.2)	416 sh, 532 (0.3), 573 (1.6), 613 (1.8)
	[Mn^{III}(OClO$_3$)(TPP)]	TOL	388 (1.2)	408 (0.92), 432 sh, 454 sh, 482 (1.1), 516 (0.13), 570 (0.2), 605 (0.16)
	[Mn^{III}(OClO$_3$)(TPP)]	THF	463 (2.8)	381 (2.0), 403 (1.9), 432 (1.9), 556 (0.36), 600 (0.31)

[a] Extinction coefficients were calculated by chemical conversion to M^{III}Cl(TPP) through addition of HCl (1 drop, concentrated, aqueous) and comparison of relative peak heights to known values for MCl(TPP).[37] [b] Spectral samples were prepared in the presence of an approximate 10-fold excess of axial ligand. [c] Subsequent addition of traces of H$_2$O results in a shift of the Soret band to that of μ-oxo dimer, [Fe(TPP)]$_2$O (406 nm), indicating that this complex, although similar, is distinct from μ-oxo dimer.

The iron(III) imidazolate complexes are unexceptional, giving the low-spin polymer [Fe(Im)(TPP)]$_n$ when a 1:1 stoichiometry is used and the low-spin bis(imidazolate)anion [Fe(Im)$_2$(TPP)]$^-$ when excess imidazolate is used. Counterions other than Bu$_4$N$^+$ such as Li$^+$ or Na$^+$ can be used but mixtures of products (polymer and bis(imidazolate) salt) may result particularly in the case of Na$^+$, presumably because of relatively similar solubilities and/or relatively slow ligand-dissociation rates. Only with the extremely sterically hindered ligand, 4,5-diphenyl-2-methylimidazolate, have we been able to prevent six-coordination. The resulting five-coordinate complex, Fe(4,5-DiPh-2-MeIm)(TPP), is high-spin (μ_{eff} = 6.2 μ_B) like most FeX(TPP) derivatives except where X is a very weak field anion;[13] this shows that even this highly hindered imidazolate has a field strength at least comparable to iodide. The driving force for the formation of this complex must be charge neutralization which, as we have recently emphasized, is very strong in ferric porphyrins.[13] Further, we find no solution spectral evidence for coordination of 4,5-diphenyl-2-methylimidazole to Fe(OClO$_3$)(TPP). The complex defies construction with space-filling models which, although such models can exaggerate bumping interactions, suggests that a severely distorted structure must exist in the 4,5-diphenyl-2-methylimidazolate derivative.

The manganese(III) complexes behave quite similarly to the iron(III) complexes in terms of stoichiometry and formulation but are much more interesting with respect to spin state. Moreover, we have been fortunate in discovering a means to grow single crystals of the polymer [Mn(Im)(TPP)]$_n$ large enough for X-ray analysis. All reported six-coordinate Mn(III) porphyrin complexes are high spin[30] ($\mu_{eff} \approx$ 5.1 μ_B) so that finding the bis(imidazolate) complex [Bu$_4$N][Mn(Im)$_2$(TPP)] is low spin (μ_{eff} = 3.2 μ_B) means that imidazolate is a considerably stronger field ligand than imidazole.[31] In the polymer, where the negative charge attraction of the imidazolate anion per Mn(III) atom is formally half that of [Mn(Im)$_2$(TPP)]$^-$, we find that the Mn(III) atoms are near the spin-crossover point. The manifestation of this is not, however, a simple spin equilibrium. Rather, there is an alteration of high- and low-spin states along the (Mn$_2$–Im–Mn$_1$–Im)$_n$ chain with the latter in a spin equilibrium. The value of the magnetic moment at low temperatures (μ_{eff} = 4.11 μ_B, calculated from the limiting slope of the Curie plot, Figure 4) is close to the spin-only average for alternating S = 2 and S = 1
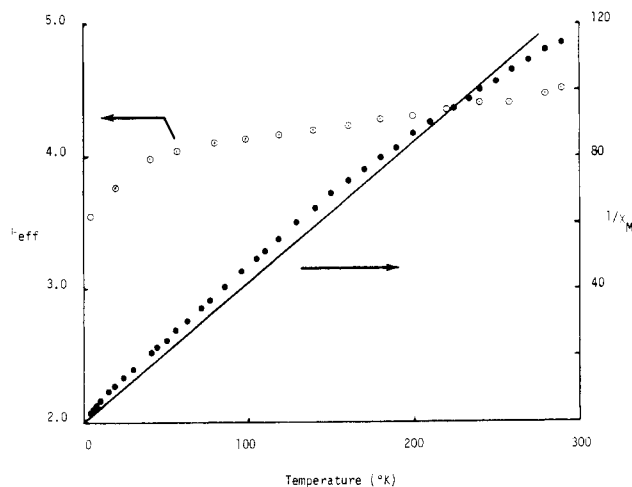

Figure 4. A graphical representation of the measured magnetic moment (μ_B) (open circles, left axis) vs. temperature, and a Curie plot ($1/\chi_M$ vs. T, solid circles, right axis) for [Mn(Im)(TPP)]$_n$. The solid line is a linear least-squares fit to the Curie plot used to illustrate the curvature in the data.

states (μ = 4.03 μ_B). Both the slight curvature of the Curie plot and the inflection in the μ_{eff} temperature profile (Figure 4) indicate that as the temperature increases the low-spin Mn(III) atom is in equilibrium with the high-spin state.[32] As is commonly the case with solid state spin equilibria a good fit of the experimental data to theory is not possible and this is made more difficult by not closely approaching the all-high-spin limit. Our estimates are that the amount of the high-spin state present at room temperature is 20–30% of the formally low-spin Mn(III) atom (i.e., 60–65% of the total Mn(III)). The curious long–long/short–short alternation of the Mn–N(Im) bond lengths revealed by the crystal structure (Figure 1) corroborates these spin-state assignments. Thus the longer pair of Mn$_2$–N(Im) bond lengths (2.280 (4) Å) are assigned to the high-spin Mn(III) atom; these lengths compare favorably to those observed in high-spin [Mn(1-MeIm)$_2$-(TPP)]ClO$_4$ where Mn–N(Im) is 2.308 (3) Å.[26] The slight shortening (~0.03 Å) can be ascribed to the increased charge attraction of an imidazolate over an imidazole. The other Mn(III)

(30) Hoard, J. L. "Porphyrins and Metalloporphyrins", Smith, K. M., Ed., Elsevier: Amsterdam, 1975; 313–380.
(31) [Mn(HIm)$_2$(TPP)]ClO$_4$·THF is high spin (μ_{eff} = 5.1 μ_B).[26]

(32) Data scatter due to the difficulty of obtaining accurate magnetic data at high temperature via the previously used "squid" technique prevented us from observing the onset of this spin equilibrium in our preliminary report.[18]

atom, however, must take a greater share of the charge attraction, resulting in shorter $Mn_1-N(Im)$ bond lengths (2.186 (5) Å) and a predominantly low-spin state. In the absence of the spin equilibrium, these axial distances would probably be slightly shorter. The observed distances can be compared to the 2.131 (14) Å Cr–N(py) bond lengths observed in the isoelectronic low-spin $Cr(py)_2(TPP)$ molecule.[33] No significant difference is expected (or observed) in the Mn–N(porph) bond distances since the $d_{x^2-y^2}$ orbital is formally unoccupied in both spin states. A spectrally evident, presumably five-coordinate Mn(III) complex (see Table VII) is formed with 4,5-diphenyl-2-methylimidazolate, but we were unable to isolate a pure product.

The manganese(II) complex with imidazolate, [Mn(Im)-(TPP)]⁻, is expectedly[20] high spin and five-coordinate. The increased field strength of imidazolate over imidazole is insufficient to cause a low-spin state and give six-coordination.

With (tetraphenylporphinato)iron(II) the spin states and stereochemistries can be manipulated in a manner similar to that of neutral imidazoles.[34] Thus, with imidazolate red, diamagnetic, low-spin, presumably six-coordinate materials are precipitated from solution. Unfortunately, their low solubilities and inconsistent elemental analyses do not allow us to distinguish between different formulations such as $[Fe(Im)_2(TPP)]^{2-}$ or $[Fe(Im)(TPP)]_n{}^{n-}$. With 2-methylimidazolate, having steric hindrance adjacent to the donor atom, the five-coordinate, high-spin complex [Fe(2-MeIm)(TPP)]⁻ can be isolated as a Bu_4N^+ salt. This complex supports the formulation of closely related protoheme species in solution where lowered CO affinities (relative to imidazole) have been reported.[6] The complex is a model for deoxyhemoglobin having a deprotonated histidine ligand. It raises the question (and should allow the experimental investigation) of whether dioxygen affinities are dramatically effected by partial or complete deprotonation of the proximal histidine ligand.

Finally, the present complexes have allowed us to increase the number of tests of what may turn out to be an observation of considerable generality, namely, anionic ligands lead to a red-shifting of the predominant Soret maximum. This has been extensively explored with anion addition to $Zn(TPP)$[35] and more recently with protoheme dimethyl ester.[6] We find that [Mn-(Im)(TPP)]⁻ has a lower energy Soret than that of both $Mn(TPP)$ and $Mn(HIm)(TPP)$. [Fe(2-MeIm)(TPP)]⁻ has a lower energy Soret than that of [Fe(2-MeHIm)(TPP)], and $[Fe(Im)_2(TPP)]^{2-}$ is lower than $Fe(HIm)_2(TPP)$. These and other comparisons are displayed pairwise in Table VII.

In conclusion, this paper explores the synthetic coordination chemistry of a variety of imidazolates with iron and manganese tetraphenylporphyrin complexes. The negative charge on the imidazolate compared to an imidazole plays a dominant role in its chemistry, increasing its ligand field strength and altering several other ligand-binding properties. In a future paper we will focus more on the exo-bidentate bridging ligand property of imidazolates.[36]

Supplementary Material Available: Figure 5, an ORTEP plot displaying the model used for disorder in the two phenyl groups associated with Mn_2, Table IV, the derived atomic coordinates and thermal parameters of the phenyl rigid groups, and listing of the observed and calculated structure amplitudes (X10) for $[Mn(Im)(TPP)]_n$ (24 pages). Ordering information is given on any current masthead page.

(33) Scheidt, W. R.; Brinegar, A. C.; Kirner, J. F.; Reed, C. A. *Inorg. Chem.* **1979**, *18*, 3610–3612.

(34) Collman, J. P.; Reed, C. A. *J. Am. Chem. Soc.* **1973**, *95*, 2048–2049.

(35) Nappa, M.; Valentine, J. S. *J. Am. Chem. Soc.* **1978**, *100*, 5075–5080.

(36) Landrum, J. T.; Grimmett, D.; Haller, K.; Scheidt, W. R.; Reed, C. A., manuscript in preparation.

(37) Boucher, L. J. *J. Am. Chem. Soc.* **1970**, *92*, 2725–2730.